JACS
JOURNAL OF THE AMERICAN CHEMICAL SOCIETY
Article
pubs.acs.org/JACS

Autocatalytic Formation of an Iron(IV)−Oxo Complex via Scandium Ion-Promoted Radical Chain Autoxidation of an Iron(II) Complex with Dioxygen and Tetraphenylborate

Yusuke Nishida,[†] Yong-Min Lee,[‡] Wonwoo Nam,*[,‡] and Shunichi Fukuzumi*[,†,‡]

[†]Department of Material and Life Science, Graduate School of Engineering, Osaka University, ALCA, Japan Science and Technology (JST), Suita, Osaka 565-0871, Japan

[‡]Department of Chemistry and Nano Science, Department of Bioinspired Science, Center for Biomimetic Systems, Ewha Womans University, Seoul 120-750, Korea

Supporting Information

ABSTRACT: A non-heme iron(IV)−oxo complex, $[(TMC)Fe^{IV}(O)]^{2+}$ (TMC = 1,4,8,11-tetramethyl-1,4,8,11-tetraazacyclotetradecane), was formed by oxidation of an iron(II) complex ($[(TMC)Fe^{II}]^{2+}$) with dioxygen (O_2) and tetraphenylborate (BPh_4^-) in the presence of scandium triflate ($Sc(OTf)_3$) in acetonitrile at 298 K via autocatalytic radical chain reactions rather than by a direct O_2 activation pathway. The autocatalytic radical chain reaction is initiated by scandium ion-promoted electron transfer from BPh_4^- to $[(TMC)Fe^{IV}(O)]^{2+}$ to produce phenyl radical ($Ph^•$). The chain propagation step is composed of the addition of O_2 to $Ph^•$ and the reduction of the resulting phenylperoxyl radical ($PhOO^•$) by scandium ion-promoted electron transfer from BPh_4^- to $PhOO^•$ to produce phenyl hydroperoxide (PhOOH), accompanied by regeneration of phenyl radical. PhOOH reacts with $[(TMC)Fe^{II}]^{2+}$ to yield phenol (PhOH) and $[(TMC)Fe^{IV}(O)]^{2+}$. Biphenyl (Ph−Ph) was formed via the radical chain autoxidation of BPh_3 by O_2. The induction period of the autocatalytic radical chain reactions was shortened by addition of a catalytic amount of $[(TMC)Fe^{IV}(O)]^{2+}$, whereas addition of a catalytic amount of ferrocene that can reduce $[(TMC)Fe^{IV}(O)]^{2+}$ resulted in elongation of the induction period. Radical chain autoxidation of BPh_4^- by O_2 also occurred in the presence of $Sc(OTf)_3$ without $[(TMC)Fe^{IV}(O)]^{2+}$, initiating the autocatalytic oxidation of $[(TMC)Fe^{II}]^{2+}$ with O_2 and BPh_4^- to yield $[(TMC)Fe^{IV}(O)]^{2+}$. Thus, the general view for formation of non-heme iron(IV)−oxo complexes via O_2-binding iron species (e.g., $Fe^{III}(O_2^{•-})$) without contribution of autocatalytic radical chain reactions should be viewed with caution.

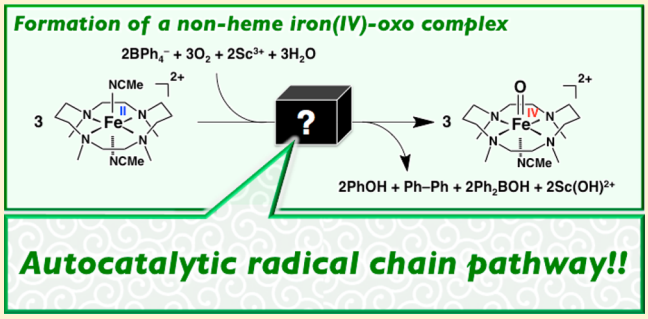

INTRODUCTION

Iron(IV)−oxo intermediates in enzymatic reactions are formed by the reductive activation of dioxygen (O_2) with two electrons and two protons.[1−3] Synthetic model compounds of such high-valent iron(IV)−oxo intermediates have been reported in the reactions of heme and non-heme iron complexes with artificial oxidants such as iodosylbenzene (PhIO), *m*-chloroperoxybenzoic acid (*m*-CPBA), and hydroperoxides (H_2O_2 and ROOH) via a so-called "shunt" pathway.[4−7] Alternatively, iron(IV)−oxo complexes ($Fe^{IV}(O)$) can be synthesized via electron-transfer oxidation with H_2O,[7−12] O_2 activation with electron and proton sources, or C−H activation by putative iron(III)−superoxo species.[13−16]

Very recently, Que and co-workers reported formation of a non-heme iron(IV)−oxo complex, $[(TMC)Fe^{IV}(O)]^{2+}$ (TMC = 1,4,8,11-tetramethyl-1,4,8,11-tetraazacyclotetradecane),[17] from the corresponding iron(II) complex, $[(TMC)Fe^{II}]^{2+}$, with O_2 and tetraphenylborate (BPh_4^-) as an electron source in the presence of Sc^{3+} ion.[18] The reaction has been proposed to occur by the formation of an iron(III)−superoxo species, $[(TMC)Fe^{III}(O_2^{•-})]^{2+}$, in the reaction of $[(TMC)Fe^{II}]^{2+}$ and O_2, followed by electron transfer from BPh_4^- to the iron(III)−superoxo complex to produce an iron(III)−peroxo complex, $[(TMC)Fe^{III}(O_2)]^+$, which is further reduced by BPh_4^- with Sc^{3+} to yield $[(TMC)Fe^{IV}(O)]^{2+}$ via the O−O bond cleavage (Scheme 1).[18] However, neither the formation of the iron(III)−superoxo and −peroxo complexes as intermediates

Scheme 1. Proposed Mechanism for Formation of $Fe^{IV}(O)$ via Reductive Activation of O_2[18]

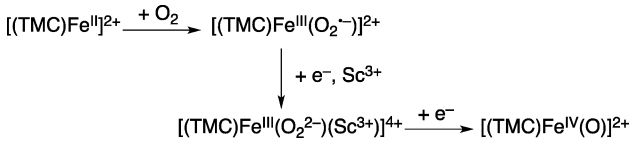

Received: March 18, 2014
Published: May 8, 2014

   dx.doi.org/10.1021/ja502732p | J. Am. Chem. Soc. 2014, 136, 8042−8049

nor the role of Sc^{3+} ion has so far been clarified. In addition, BPh_4^- is regarded as a weak electron donor, which is generally used as an electron donor in photoinduced electron-transfer reactions.[19,20] Thus, it is quite unlikely that BPh_4^- acts as an effective electron donor in the proposed mechanism (Scheme 1).

We therefore reinvestigated the O_2 activation reaction by $[(TMC)Fe^{II}]^{2+}$ and BPh_4^- in the presence of Sc^{3+} ion, especially to understand the role of the Sc^{3+} ion binding to an iron(III)−peroxo complex in the O_2 activation process.[18,21] Interestingly, we found that the formation of $[(TMC)Fe^{IV}(O)]^{2+}$ in the reaction of $[(TMC)Fe^{II}]^{2+}$ and O_2 in the presence of Sc^{3+} ion does not occur via a simple electron-transfer reaction as shown in Scheme 1 but via Sc^{3+} ion-promoted radical chain autoxidation pathways, which are autocatalyzed by the product ($[(TMC)Fe^{IV}(O)]^{2+}$). We report herein detailed mechanistic studies that unveil the roles of BPh_4^- and Sc^{3+} ion in the generation of a high-valent iron(IV)−oxo complex in the reaction of a non-heme iron catalyst and O_2.

■ RESULTS AND DISCUSSION

Autocatalytic Formation of $[(TMC)Fe^{IV}(O)]^{2+}$. As reported previously by Que and co-workers,[18] $[(TMC)Fe^{II}]^{2+}$ was oxidized by O_2 in the presence of $Sc(OTf)_3$ and $NaBPh_4$ in O_2-saturated MeCN as shown in Figure 1, where formation of

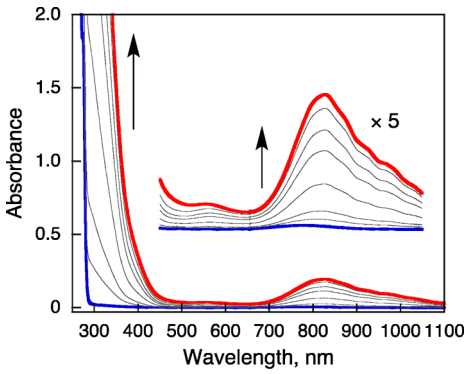

Figure 1. Absorption spectral changes observed in formation of $[(TMC)Fe^{IV}(O)]^{2+}$ in the reaction of $[(TMC)Fe^{II}]^{2+}$ (0.50 mM) with $NaBPh_4$ (1.0 mM), and $Sc(OTf)_3$ (1.0 mM) in O_2-saturated MeCN at 298 K.

$[(TMC)Fe^{IV}(O)]^{2+}$ was observed as an increase in the absorption band at 820 nm. The time course of the reaction was monitored by an increase in absorbance at 820 nm due to $[(TMC)Fe^{IV}(O)]^{2+}$ as shown in Figure 2, which exhibits a sigmoidal curve with an induction period, which was not recognized previously.[18] When a catalytic amount of the product ($[(TMC)Fe^{IV}(O)]^{2+}$) was added to a reaction solution, the induction period was shortened with increasing concentration of $[(TMC)Fe^{IV}(O)]^{2+}$ as shown in Figure 2, where the steady-state rate after the induction period was nearly the same irrespective of the initial concentration of $[(TMC)Fe^{IV}(O)]^{2+}$ (the reason is discussed later). Such an autocatalytic behavior was confirmed by the effect of a catalytic amount of Fc which can reduce $[(TMC)Fe^{IV}(O)]^{2+}$ as shown in Figure 3, where the induction period increased with an increase in concentration of Fc. Fc is known to act as an electron donor to reduce $[(TMC)Fe^{IV}(O)]^{2+}$.[22,23] After Fc was consumed, the reaction started rapidly without any induction period (Figure 3).

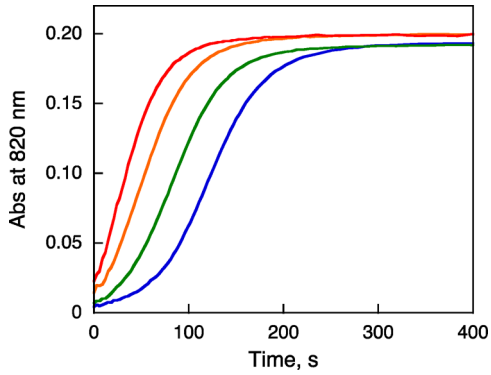

Figure 2. Time courses of absorption change monitored at 820 nm for formation of $[(TMC)Fe^{IV}(O)]^{2+}$ in reactions of $[(TMC)Fe^{II}]^{2+}$ (0.50 mM) with $NaBPh_4$ (1.0 mM) and $Sc(OTf)_3$ (1.0 mM) in the absence and presence of a catalytic amount of $[(TMC)Fe^{IV}(O)]^{2+}$ (blue, 0 M; green, 10 μM; orange, 25 μM; red, 50 μM) in O_2-saturated MeCN at 298 K. The reaction was started by adding $Sc(OTf)_3$ to an O_2-saturated MeCN solution of $[(TMC)Fe^{II}]^{2+}$ and $NaBPh_4$.

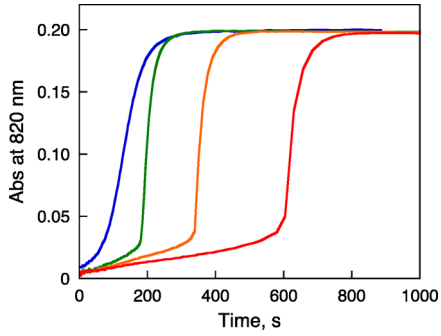

Figure 3. Time courses of absorbance at 820 nm for formation of $[(TMC)Fe^{IV}(O)]^{2+}$ in reactions of $[(TMC)Fe^{II}]^{2+}$ (0.50 mM) with $NaBPh_4$ (1.0 mM) and $Sc(OTf)_3$ (1.0 mM) in the absence and presence of a catalytic amount of Fc (blue, 0 M; green, 10 μM; orange, 25 μM; red, 50 μM) in O_2-saturated MeCN at 298 K.

The spectral titration for formation of $[(TMC)Fe^{IV}(O)]^{2+}$ in the oxidation of $[(TMC)Fe^{II}]^{2+}$ with different concentrations of BPh_4^- and a fixed concentration of Sc^{3+} ion in O_2-saturated MeCN is shown in Figure 4, which indicates that less than 1 equiv of BPh_4^- is enough to produce $[(TMC)Fe^{IV}(O)]^{2+}$ with 97% yield. The spectral titration for formation of $[(TMC)Fe^{IV}(O)]^{2+}$ in the oxidation of $[(TMC)Fe^{II}]^{2+}$ was also

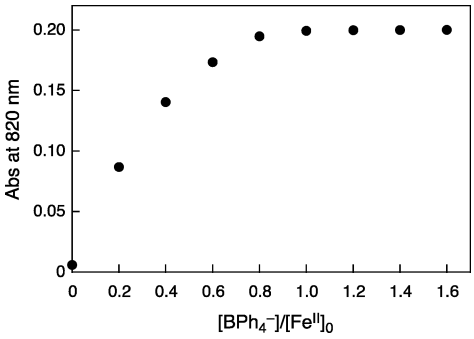

Figure 4. Plot of absorbance at 820 nm vs ratio of BPh_4^- to $[(TMC)Fe^{II}]^{2+}$ for formation of $[(TMC)Fe^{IV}(O)]^{2+}$ in reaction of $[(TMC)Fe^{II}]^{2+}$ (0.50 mM) with $NaBPh_4$ and $Sc(OTf)_3$ (1.0 mM) in O_2-saturated MeCN at 298 K.

dx.doi.org/10.1021/ja502732p | J. Am. Chem. Soc. 2014, 136, 8042−8049

performed with different concentrations of Sc^{3+} and a fixed concentration of BPh_4^- in O_2-saturated MeCN as shown in Figure 5, which indicates that less than 1 equiv of Sc^{3+} is also

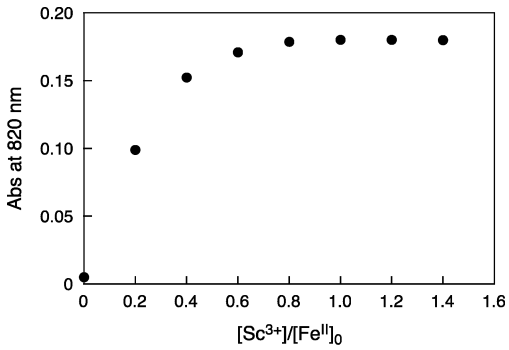

Figure 5. Plot of absorbance at 820 nm vs ratio of Sc^{3+} to $[(TMC)Fe^{II}]^{2+}$ for formation of $[(TMC)Fe^{IV}(O)]^{2+}$ in reaction of $[(TMC)Fe^{II}]^{2+}$ (0.50 mM) with $NaBPh_4$ (1.0 mM) and $Sc(OTf)_3$ in O_2-saturated MeCN at 298 K.

enough to produce $[(TMC)Fe^{IV}(O)]^{2+}$. The ^1H NMR spectrum of an O_2-saturated CD_3CN solution after the oxidation of $[(TMC)Fe^{II}]^{2+}$ with BPh_4^- and Sc^{3+} is shown in Figure S1 in Supporting Information. By comparison of ^1H NMR spectra of authentic samples, the product yields based on the amount of BPh_4^- were determined as phenol (PhOH, 95%), biphenyl (Ph−Ph, 56%), triphenylborane (Ph_3B, 20%), and diphenylborinic acid (Ph_2BOH, 78%).[24,25] The ^1H NMR spectra of authentic compounds are shown in Figure S2 (Supporting Information). The formation of phenol and biphenyl was also confirmed by gas chromatography−mass spectrometry (GC−MS) (see Experimental Section and Figure S3 in Supporting Information).

Autocatalytic Radical Chain Mechanism. The formation of phenol can be explained by the autocatalytic radical chain reactions in Scheme 2.[26] The initiation step may be Sc^{3+}-

Scheme 2. Sc^{3+}-Promoted Electron-Transfer Chain Reactions for Formation of $[(TMC)Fe^{IV}(O)]^{2+}$ in Reaction of $[(TMC)Fe^{II}]^{2+}$ with O_2 and BPh_4^-

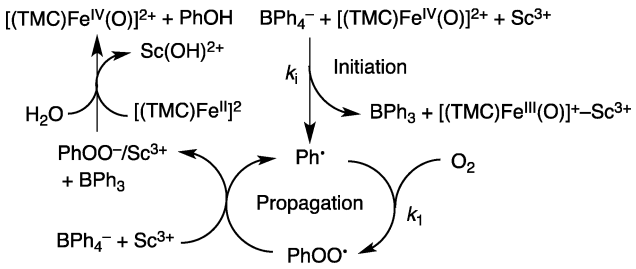

promoted electron transfer from BPh_4^- to $[(TMC)Fe^{IV}(O)]^{2+}$ to produce Ph•, BPh_3, and the $[(TMC)Fe^{III}(O)]^+$−Sc^{3+} complex.[27−31] Phenyl radical (Ph•) is known to react rapidly with O_2 to produce the peroxyl radical (PhOO•).[32,33] Then, Sc^{3+}-promoted electron transfer from BPh_4^- to PhOO• may occur as a propagation step to produce BPh_3 and the $PhOO^-/Sc^{3+}$ complex, accompanied by regeneration of Ph•. The $PhOO^-/Sc^{3+}$ complex reacts with $[(TMC)Fe^{II}]^{2+}$ to produce $[(TMC)Fe^{IV}(O)]^{2+}$ and PhOH after the reaction with residual water (Scheme 2). The stoichiometry of the reaction in Scheme 2 is given by eq 1, which can explain the formation of PhOH and Ph_3B. However, the yield of Ph_3B (20%) is much less than that expected from eq 1 (100%) and the formation of Ph−Ph is not included in eq 1.

$$[(TMC)Fe^{II}]^{2+} + BPh_4^- + O_2 + Sc^{3+} + H_2O \rightarrow [(TMC)Fe^{IV}(O)]^{2+} + PhOH + BPh_3 + Sc(OH)^{2+} \quad (1)$$

The biphenyl (Ph−Ph) may be produced by radical coupling of Ph•. However, such radical coupling reaction acts as a termination step for the radical chain reactions in Scheme 2. The maximum chain length is evaluated as the ratio of the maximum rate of formation of $[(TMC)Fe^{IV}(O)]^{2+}$ to the slow decay rate of $[(TMC)Fe^{IV}(O)]^{2+}$ at prolonged reaction time (Figure 6) to be 290, because the decay rate of [(TMC)-

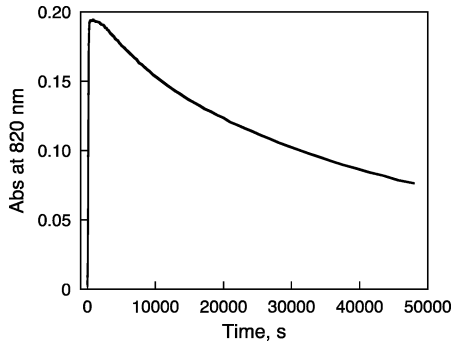

Figure 6. Time profiles of absorbance at 820 nm after formation of $[(TMC)Fe^{IV}(O)]^{2+}$ in reaction of $[(TMC)Fe^{II}]^{2+}$ (0.50 mM) with $NaBPh_4$ (1.0 mM) and $Sc(OTf)_3$ (1.0 mM) in O_2-saturated MeCN at 298 K.

$Fe^{IV}(O)]^{2+}$, which corresponds to the initiation step (i.e., Sc^{3+}-promoted electron transfer from BPh_4^- to $[(TMC)Fe^{IV}(O)]^{2+}$), is equal to the rate of the termination step under steady-state conditions in Scheme 2. Such a large chain length indicates that the radical coupling of Ph• is not the main pathway for formation of Ph−Ph, which must be a product of the chain propagation step. In this context, it is well-known that the oxidation of organoboranes by O_2 occurs via radical chain autoxidation reactions.[34,35] Thus, further autoxidation of Ph_3B may occur as shown in Scheme 3, where Ph• reacts with Ph_3B to produce Ph−Ph and Ph_2B•. Ph_2B• reacts further with O_2 to

Scheme 3. Radical Chain Mechanism for Formation of Ph−Ph and $[(TMC)Fe^{IV}(O)]^{2+}$ via Autoxidation of Ph_3B

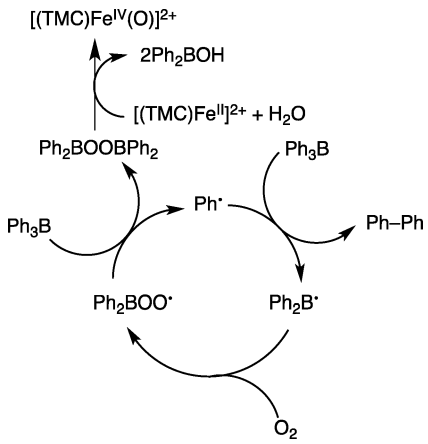

produce the peroxyl radical ($Ph_2BOO^{\bullet}$), which reacts with Ph_3B to produce $Ph_2BOOBPh_2$, accompanied by regeneration of $Ph^{\bullet}$. Then, the peroxide ($Ph_2BOOBPh_2$) oxidizes $[(TMC)Fe^{II}]^{2+}$ to produce $[(TMC)Fe^{IV}(O)]^{2+}$. The stoichiometry of the reaction in Scheme 3 is given by eq 2. By combining eqs 1 and 2, the overall stoichiometry is given by eq 3, which indicates that $[(TMC)Fe^{IV}(O)]^{2+}$ is produced by using less than 1 equiv of BPh_4^- and Sc^{3+} (Figures 4 and 5).

$$[(TMC)Fe^{II}]^{2+} + 2BPh_3 + O_2 + H_2O \rightarrow [(TMC)Fe^{IV}(O)]^{2+} + Ph{-}Ph + 2Ph_2BOH \quad (2)$$

$$3[(TMC)Fe^{II}]^{2+} + 2BPh_4^- + 3O_2 + 2Sc^{3+} + 3H_2O \rightarrow 3[(TMC)Fe^{IV}(O)]^{2+} + Ph{-}Ph + 2PhOH + 2Ph_2BOH + 2Sc(OH)^{2+} \quad (3)$$

The yield of Ph−Ph (56%) is consistent with eq 2. Diphenylborinic acid (Ph_2BOH) may be produced by the hydrolysis of Ph_2BOBPh_2. Biphenyl (Ph−Ph) may also be produced by the chain termination reaction (radical coupling) in Schemes 1 and 2. However, the contribution of the termination step may be negligible judging from the long chain length as indicated by the effect of the catalytic amount of ferrocene to stop the autocatalytic reaction in Figure 3.

According to Schemes 2 and 3, the autocatalytic formation of $[(TMC)Fe^{IV}(O)]^{2+}$ may be composed of two steps: one is via the autocatalytic oxidation of Ph_4B^- with O_2 in the presence of Sc^{3+} (Scheme 2) and the other is via the autocatalytic oxidation of Ph_3B with O_2 in the absence of Sc^{3+} (Scheme 3). The two-step time course of the formation of $[(TMC)Fe^{IV}(O)]^{2+}$ is shown in Figure 7, where the fast component corresponds to

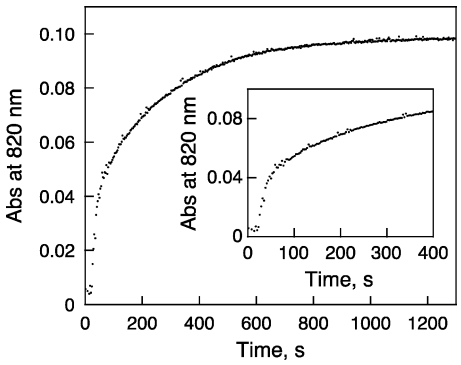

Figure 7. Time profile of absorbance at 820 nm due to $[(TMC)Fe^{IV}(O)]^{2+}$ in reaction of $[(TMC)Fe^{II}]^{2+}$ (0.50 mM) with $NaBPh_4$ (1.0 mM) and $Sc(OTf)_3$ (0.10 mM) in O_2-saturated MeCN at 298 K. The initial change is shown in the inset.

the formation of $[(TMC)Fe^{IV}(O)]^{2+}$ (0.10 mM) by the reaction of $[(TMC)Fe^{II}]^{2+}$ (0.50 mM) with BPh_4^- (1.0 mM) and $Sc(OTf)_3$ (0.10 mM) (eq 1), followed by the slower increase in absorbance at 820 nm due to $[(TMC)Fe^{IV}(O)]^{2+}$ after consumption of Sc^{3+} (eq 2).

In order to trap $Ph^{\bullet}$, a catalytic amount of isopentyl nitrite was added to an MeCN solution of $[(TMC)Fe^{II}]^{2+}$, $NaBPh_4$, and $Sc(OTf)_3$ as shown in Figure 8, because isopentyl nitrite is known to act as a radical trap.[36] To our surprise, the induction period became shorter with increasing catalytic amount of isopentyl nitrite. Thus, isopentyl nitrite acts as an initiator rather than as a radical trap probably due to Sc^{3+}-promoted

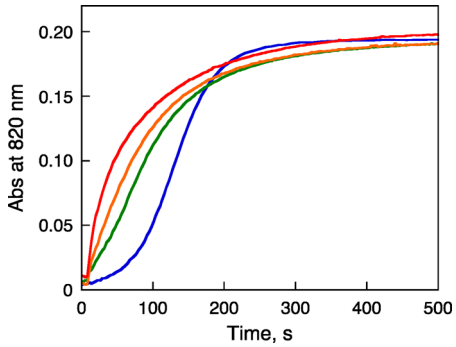

Figure 8. Time profiles of absorbance at 820 nm in reactions of $[(TMC)Fe^{II}]^{2+}$ (0.50 mM) with $NaBPh_4$ (1.0 mM) and $Sc(OTf)_3$ (1.0 mM) in the absence and presence of a catalytic amount of isopentyl nitrite (blue, 0 M; green, 10 μM; orange, 25 μM; red, 50 μM) in O_2-saturated MeCN at 298 K.

electron transfer from BPh_4^- to isopentyl nitrite. On the other hand, addition of a catalytic amount of tetramethyl-*p*-benzoquinone retarded the formation of $[(TMC)Fe^{IV}(O)]^{2+}$ as shown in Figure S4 (Supporting Information), probably due to the radical trap of the chain carrier in Schemes 2 and 3.

In order to determine the rate-determining step in the autocatalytic formation of $[(TMC)Fe^{IV}(O)]^{2+}$ in Schemes 2 and 3, the effects of concentrations of $NaBPh_4$, $Sc(OTf)_3$, and O_2 on the rate of formation of $[(TMC)Fe^{IV}(O)]^{2+}$ were examined as shown in Figures S5, S6, and S7, respectively, of the Supporting Information. The steady-state rate of formation of $[(TMC)Fe^{IV}(O)]^{2+}$ was proportional to concentrations of $NaBPh_4$, $Sc(OTf)_3$, and O_2 (Figures S5, S6, and S7, respectively, of the Supporting Information).[37] Such dependence of the steady-state rate of $[(TMC)Fe^{IV}(O)]^{2+}$ on concentrations of $NaBPh_4$, $Sc(OTf)_3$, and O_2 suggests that the rate-determining step in Scheme 2 may be the reaction of $Ph^{\bullet}$ with O_2, because this is the only step, the rate of which is proportional to O_2 concentration. In such a case the rate of formation of $[(TMC)Fe^{IV}(O)]^{2+}$ is the same as the rate of the reaction of $Ph^{\bullet}$ with O_2 as given by eq 4,

$$d[Fe^{IV}(O)]/dt = k_1[Ph^{\bullet}][O_2] \quad (4)$$

where k_1 is the rate constant of the addition of O_2 to $Ph^{\bullet}$ in Scheme 2. Because $[(TMC)Fe^{IV}(O)]^{2+}$ has a radical character such as $[(TMC)Fe^{III}{-}O^{\bullet}]^{2+}$, the termination reaction of $Ph^{\bullet}$ in the radical chain reactions in Scheme 2 may be the radical coupling between $[(TMC)Fe^{III}{-}O^{\bullet}]^{2+}$ and $Ph^{\bullet}$ to produce $[(TMC)Fe^{III}{-}(OPh)]^{2+}$ as shown in eq 5,

$$[(TMC)Fe^{IV}(O)]^{2+} + Ph^{\bullet} \xrightarrow{k_t} [(TMC)Fe^{III}(OPh)]^{2+} \quad (5)$$

where k_t is the rate constant of the termination reaction. Under the steady-state conditions, the rate of the initiation (R_i) should be the same as the rate of termination as given by eq 6,

$$R_i = k_i[Fe^{IV}(O)][BPh_4^-][Sc^{3+}] = k_t[Fe^{IV}(O)][Ph^{\bullet}] \quad (6)$$

where k_i is the rate constant of the initiation reaction in Scheme 2, which is proportional to concentrations of BPh_4^- and Sc^{3+}. From eq 6, eq 4 is rewritten by eq 7,

$$d[Fe^{IV}(O)]/dt = k_1(k_i/k_t)[BPh_4^-][Sc^{3+}][O_2] \quad (7)$$

which agrees with the experimental results in Figure 2, where the steady-state rate was independent of the initial concen-

tration of $[(TMC)Fe^{IV}(O)]^{2+}$, and also the observed dependence of the steady-state rate on concentrations of $NaBPh_4$, $Sc(OTf)_3$, and O_2 in Figures S5–S7 in the Supporting Information.

Initiation of Autocatalytic Radical Chain Reactions. In Schemes 2 and 3, the initiation step is Sc^{3+}-promoted electron transfer from BPh_4^- to $[(TMC)Fe^{IV}(O)]^{2+}$. Then, a question arises: what is the initiation step in the absence of $[(TMC)Fe^{IV}(O)]^{2+}$ for the autocatalytic reactions? It was found that the autoxidation of BPh_4^- by O_2 occurred in the presence of Sc^{3+} without $[(TMC)Fe^{II}]^{2+}$ as shown by ^{1}H NMR spectra of the products in Figure S8 (Supporting Information).[38] In this case, not only PhOH and Ph–Ph but also Ph–H were produced. The time course of the autoxidation of BPh_4^- by O_2 occurred in the presence of Sc^{3+} as shown in Figure 9. The amount of

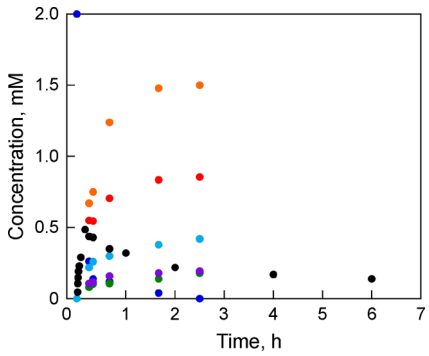

Figure 9. Time profiles of autoxidation of $NaBPh_4$ (2.0 mM, blue) in the presence of $Sc(OTf)_3$ (4.0 mM) in O_2-saturated MeCN at 298 K to form BPh_3 (green), PhOH (orange), Ph–Ph (red), Ph_2BOH (sky blue), Ph–H (purple), and PhOOH (black).

PhOOH produced during the autoxidation was determined by the iodometric titration as shown in Figure S9 (Supporting Information).[39] It should be noted that no autoxidation of BPh_4^- by O_2 occurred in the absence of Sc^{3+}. Thus, the initiation may be started by Sc^{3+}-promoted electron transfer from BPh_4^- to O_2 to produce $Ph^\bullet$, Ph_3B, and the $O_2^{\bullet-}$–Sc^{3+} complex. In the propagation step, $Ph^\bullet$ reacts with O_2 to produce $PhOO^\bullet$, followed by Sc^{3+}-promoted electron transfer from BPh_4^- to $PhOO^\bullet$ with residual water to produce Ph_3B, PhOOH, and $Sc(OH)^{2+}$, accompanied by regeneration of $Ph^\bullet$ (Scheme 4). The overall stoichiometry of Scheme 4 is given by eq 8.

$$BPh_4^- + O_2 + Sc^{3+} + H_2O \rightarrow BPh_3 + PhOOH + Sc(OH)^{2+} \quad (8)$$

Scheme 4. Radical Chain Mechanism for Sc^{3+}-Promoted Autoxidation of BPh_4^- by O_2 without $[(TMC)Fe^{II}]^{2+}$

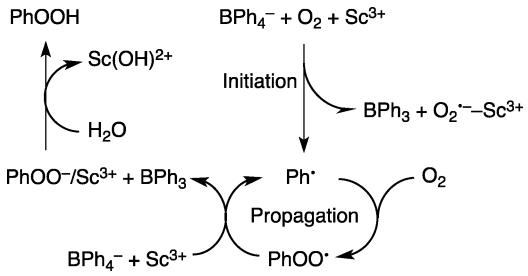

PhOOH may decompose via radical chain reactions in Scheme 5.[40] The bimolecular reaction of $PhOO^\bullet$ produces 2

Scheme 5. Radical Chain Mechanism for Decomposition of PhOOH to PhOH

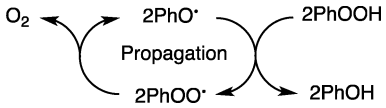

equiv of $PhO^\bullet$ and 1 equiv of O_2. $PhO^\bullet$ abstracts hydrogen from PhOOH to produce PhOH, accompanied by regeneration of $PhOO^\bullet$ (Scheme 5). The stoichiometry of the radical chain reactions in Scheme 5 is given by eq 9.

$$2PhOOH \rightarrow 2PhOH + O_2 \quad (9)$$

By combining eqs 8 and 9, the overall stoichiometry is given by eq 10.

$$2BPh_4^- + O_2 + 2Sc^{3+} + 2H_2O \rightarrow 2BPh_3 + 2PhOH + 2Sc(OH)^{2+} \quad (10)$$

According to eq 10, the expected yields of BPh_3 and PhOH are 100%. However, the observed yield of BPh_3 (9%) is much smaller than the expected yield (100%), whereas the observed yield of PhOH (75%) is close to the expected yield.

The much smaller yield of BPh_3 may result from the further autoxidation of BPh_3 by O_2 in Scheme 3, where BPh_3 is converted to yield Ph–Ph (43% yield). In the absence of $[(TMC)Fe^{II}]^{2+}$, $Ph_2BOOBPh_2$ may be converted to Ph_2BOH (21% yield) via the radical chain decomposition and hydrolysis (Scheme 6). The overall stoichiometry of Scheme 6 is given by

Scheme 6. Radical Chain Mechanism for Decomposition of $Ph_2BOOBPh_2$ to Form Ph_2BOH

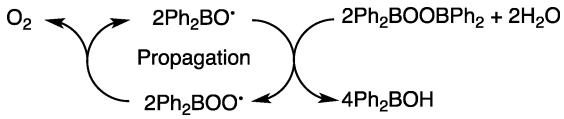

eq 11. The smaller yield of Ph_2BOH than that expected from eq 11 may result from the further autoxidation of Ph_2BOH by O_2.

$$2BPh_3 + 1/2O_2 + H_2O \rightarrow Ph–Ph + 2Ph_2BOH \quad (11)$$

The formation of Ph–H can be explained by the radical chain reactions in Scheme 7, where $Ph^\bullet$ reacts with PhOOH to produce Ph–H, accompanied by regeneration of $PhOO^\bullet$. This is followed by Sc^{3+}-promoted electron transfer from BPh_4^- to $PhOO^\bullet$ with residual water to produce Ph_3B and $Sc(OH)^{2+}$, accompanied by regeneration of $Ph^\bullet$ and PhOOH (Scheme 7).

Scheme 7. Radical Chain Mechanism for Formation of Ph–H from BPh_4^- with Sc^{3+}

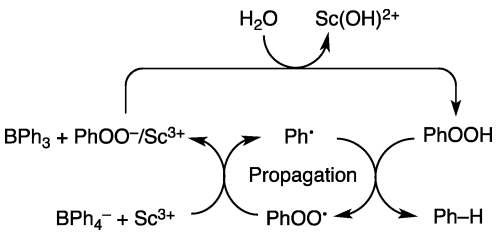

dx.doi.org/10.1021/ja502732p | J. Am. Chem. Soc. 2014, 136, 8042–8049

The stoichiometry of the reactions of Scheme 7 is shown in eq 12. The instability of BPh_4^- in the presence of an acid to produce Ph_3B and Ph−H has been known for a long time, although the reaction mechanism has yet to be clarified.[41]

$$2BPh_4^- + Sc^{3+} + H_2O \rightarrow Ph{-}H + BPh_3 + Sc(OH)^{2+} \quad (12)$$

Autoxidation of BPh_4^- by O_2 in the presence of Sc^{3+} produces hydroperoxide (PhOOH), which reacts with $[(TMC)Fe^{II}]^{2+}$ to produce $[(TMC)Fe^{IV}(O)]^{2+}$, to start autocatalyzed radical chain reactions in Scheme 2. The reaction time for formation of $[(TMC)Fe^{IV}(O)]^{2+}$ via the Sc^{3+}-promoted autocatalytic oxidation of $[(TMC)Fe^{II}]^{2+}$ by O_2 and BPh_4^- (Figure 2) is significantly shorter than that for Sc^{3+}-promoted autoxidation of BPh_4^- by O_2 without $[(TMC)Fe^{II}]^{2+}$. In such a case, the order of addition of reactants affects the outcome of the reaction. When $[(TMC)Fe^{II}]^{2+}$ was added to an O_2-saturated MeCN solution of $NaBPh_4$ and $Sc(OTf)_3$ after 10 min (green line in Figure 10), the rate and yield of formation of $[(TMC)Fe^{IV}(O)]^{2+}$ were significantly smaller than those when $Sc(OTf)_3$ was added to an O_2-saturated MeCN solution of $[(TMC)Fe^{II}]^{2+}$ and $NaBPh_4$ (black line in Figure 10). In the former case, the Sc^{3+}-promoted autoxidation of BPh_4^- (Schemes 4 and 5) was mostly completed before the addition of $[(TMC)Fe^{II}]^{2+}$ when the amount of unreacted BPh_4^- was not enough for the complete conversion of $[(TMC)Fe^{II}]^{2+}$ to $[(TMC)Fe^{IV}(O)]^{2+}$.[42]

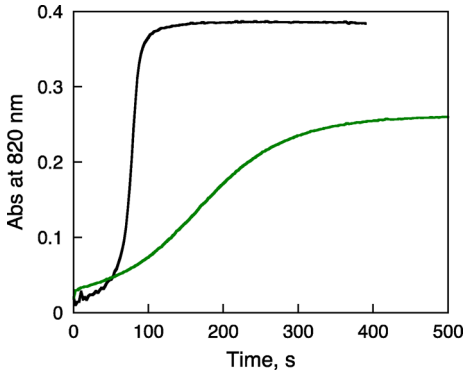

Figure 10. Time courses of absorption change monitored at 820 nm for formation of $[(TMC)Fe^{IV}(O)]^{2+}$ in reactions of $[(TMC)Fe^{II}]^{2+}$ (1.0 mM) with $NaBPh_4$ (2.0 mM) and $Sc(OTf)_3$ (4.0 mM) in O_2-saturated MeCN at 298 K. The reaction was started by adding $Sc(OTf)_3$ to an O_2-saturated MeCN solution of $[(TMC)Fe^{II}]^{2+}$ and $NaBPh_4$ (black line), whereas the reaction was started by adding $[(TMC)Fe^{II}]^{2+}$ to an O_2-saturated MeCN solution of $NaBPh_4$ and $Sc(OTf)_3$ after 10 min (green line).

As the case of the Sc^{3+}-promoted autocatalytic oxidation of $[(TMC)Fe^{II}]^{2+}$ by O_2 and BPh_4^-, the formation of $[(TMC)Fe^{IV}(O)]^{2+}$ was also promoted by triflic acid (HOTf) as shown in Figure 11. In this case as well, the rate of formation of $[(TMC)Fe^{IV}(O)]^{2+}$ when $[(TMC)Fe^{II}]^{2+}$ was added to an O_2-saturated MeCN solution of $NaBPh_4$ and HOTf after 10 min (red line in Figure 11) was significantly slower than that when HOTf was added to an O_2-saturated MeCN solution of $[(TMC)Fe^{II}]^{2+}$ and $NaBPh_4$ (blue line in Figure 11). The yield of $[(TMC)Fe^{IV}(O)]^{2+}$ was much lower when the addition time of $[(TMC)Fe^{II}]^{2+}$ was elongated to 26 h (green line in Figure 11). Thus, in the case of HOTf as well the acid-promoted autoxidation of BPh_4^- by O_2 occurred before the acid-promoted formation of $[(TMC)Fe^{IV}(O)]^{2+}$ via the acid-promoted autocatalytic oxidation of $[(TMC)Fe^{II}]^{2+}$ by O_2 and BPh_4^-.[43−45]

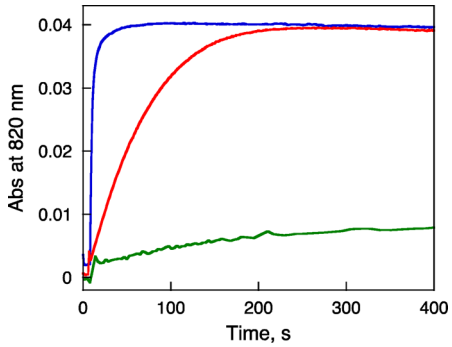

Figure 11. Time courses of absorption change monitored at 820 nm for formation of $[(TMC)Fe^{IV}(O)]^{2+}$ in reaction of $[(TMC)Fe^{II}]^{2+}$ (0.10 mM) with $NaBPh_4$ (1.0 mM) and HOTf (1.0 mM) in O_2-saturated MeCN at 298 K. The reaction was initiated by adding HOTf to an O_2-saturated MeCN solution of $[(TMC)Fe^{II}]^{2+}$ and $NaBPh_4$ (blue line), whereas the reaction was initiated by adding $[(TMC)Fe^{II}]^{2+}$ to an O_2-saturated MeCN solution of $NaBPh_4$ and HOTf after 10 min (red line) and after 26 h (green line).

■ CONCLUSION

In summary, we have demonstrated that formation of a non-heme iron(IV)−oxo complex by reductive O_2 activation with BPh_4^- and Sc^{3+} ions proceeds via autocatalytic radical chain reactions, in which $PhOO^\bullet$ is the chain carrier to produce the peroxide−Sc^{3+} complex ($PhOO^-/Sc^{3+}$) that reacts with $[(TMC)Fe^{II}]^{2+}$ to yield $[(TMC)Fe^{IV}(O)]^{2+}$. The autoxidation of BPh_4^- is initiated by Sc^{3+}-promoted electron transfer from BPh_4^- to $[(TMC)Fe^{IV}(O)]^{2+}$ to produce $Ph^\bullet$, to which O_2 is added to afford the chain carrier radical ($PhOO^\bullet$). Thus, $[(TMC)Fe^{IV}(O)]^{2+}$ is produced via an autocatalytic radical chain reaction (Scheme 2) rather than via a direct reductive O_2 activation (Scheme 1). Such autocatalytic radical chain pathways may be generally operative when weak electron donors such as BPh_4^- are employed as an electron source for the generation of high-valent metal−oxo species with O_2 and acids. Thus, the present study provides general caution for investigating the formation of high-valent metal−oxo complexes via O_2 activation without considering the possible contribution of autocatalytic radical chain pathways.

■ EXPERIMENTAL SECTION

Materials. Commercially available chemicals were used without further purification unless otherwise indicated. Solvents were dried according to published procedures and distilled under N_2 prior to use.[46] Iodosylbenzene (PhIO) was prepared by a literature method.[47] Sodium tetraphenylborate ($NaBPh_4$), phenylboronic acid ($PhB(OH)_2$), and trifric acid (HOTf) were purchased from Tokyo Chemical Industry Co., Ltd. Scandium triflate ($Sc(OTf)_3$), triphenylborane (BPh_3), biphenyl (Ph−Ph), and ferrocene (Fc) were purchased from Aldrich Chemical. Phenol (PhOH), benzene (Ph−H), and sodium iodide (NaI) were purchased from Wako Pure Chemical Industries, Ltd. Deuterated [$^2H_3$]acetonitrile (CD_3CN) was purchased from Euri SO-TOP, CEA, France. Dichloroethane and TMC ligand were purchased from Aldrich Chemical. Iron complexes, $[(TMC)Fe^{II}(CH_3CN)_2](CF_3SO_3)_2$, and $[(TMC)Fe^{IV}(O)]^{2+}$, were prepared by literature methods.[17]

Kinetic Measurements. Kinetic measurements were performed on a Hewlett-Packard 8453 spectrophotometer using a quartz cuvette (path length = 10 mm) at 298 K. Typically, the formation reaction of

$[(TMC)Fe^{IV}(O)]^{2+}$ was started by adding $Sc(OTf)_3$ (1.0 mM) into O_2-saturated MeCN in the presence of $[(TMC)Fe^{II}]^{2+}$ and $NaBPh_4$ with other additives such as $[(TMC)Fe^{IV}(O)]^{2+}$, ferrocene, isopentyl nitrite, and tetramethyl-*p*-benzoquinone.

Iodometric Titrations. A 100 μL volume of the reacting O_2-saturated MeCN solution of $NaBPh_4$ (2.0 mM) and $Sc(OTf)_3$ (4.0 mM) was added to 2.0 mL of NaI-saturated MeCN solution. The amount of formed PhOOH was calculated by monitoring the appearance of an absorption band at 361 nm due to the corresponding triiodide ion (I_3^-; λ_{max} 361 nm, $\varepsilon_{max} = 2.5 \times 10^4$ M^{-1} cm^{-1}).[39]

NMR and GC−MS Measurements. Nuclear magnetic resonance (NMR) detection of BPh_3, PhOH, Ph−Ph, Ph_2BOH, $PhB(OH)_2$, and Ph−H was performed as follows: an O_2-saturated MeCN-d_3 solution of $Sc(OTf)_3$ (4.0 mM) was added to an O_2-saturated MeCN-d_3 solution of $[(TMC)Fe^{II}]^{2+}$ (2.0 mM) and $NaBPh_4$ (1.0 mM) or to an O_2-saturated MeCN-d_3 solution of $NaBPh_4$ (2.0 mM). After 10 min, ^1H NMR spectra were recorded on a JEOL JMN-AL-300 NMR spectrometer at room temperature. Products were quantified by comparison of ^1H NMR spectra with that of dichloroethane (2.0 mM) as an authentic sample. Products were also analyzed by GC−MS using a Shimadzu QP-5000 equipped with a Restek Rxi-5Sil MS (30 m, 0.25 mm i.d., 0.25 mm df) and electron impact ionization.

■ ASSOCIATED CONTENT

Supporting Information

^1H NMR spectra of O_2-saturated CD_3CN solution after oxidation of $[(TMC)Fe^{II}]^{2+}$ with $NaBPh_4$ and $Sc(OTf)_3$; of $NaBPh_4$, BPh_3, PhOH, Ph−Ph, Ph−H, and $PhB(OH)_2$ in CD_3CN; and of resulting solution obtained in reaction of $NaBPh_4$ with O_2 in the presence of $Sc(OTf)_3$. Simulation spectra of mixtures of BPh_3, Ph−Ph, PhOH, and Ph−H obtained by combining the authentic spectra of BPh_3, Ph−Ph, PhOH, and Ph−H. GC of reaction mixture obtained by the reaction of $[(TMC)Fe^{II}]^{2+}$ with $NaBPh_4$ and $Sc(OTf)_3$ in O_2-saturated MeCN at 298 K. Time profiles of the absorbance at 820 nm in the reactions of $[(TMC)Fe^{II}]^{2+}$ with $NaBPh_4$ and $Sc(OTf)_3$. Plots of steady-state rate of formation of $[(TMC)Fe^{IV}(O)]^{2+}$ vs concentration of $NaBPh_4$, $Sc(OTf)_3$, and O_2. Spectral changes due to I_3^- formation upon addition of reacting O_2-saturated MeCN solution of $NaBPh_4$ and $Sc(OTf)_3$ to NaI-saturated MeCN solution. This material is available free of charge via the Internet at http://pubs.acs.org.

■ AUTHOR INFORMATION

Corresponding Authors

fukuzumi@chem.eng.osaka-u.ac.jp
wwnam@ewha.ac.kr

Notes

The authors declare no competing financial interest.

■ ACKNOWLEDGMENTS

This work was supported by an ALCA project from JST, Japan (to S.F.) and by KRF/MEST of Korea through CRI (NRF-2012R1A3A2048842) and GRL (NRF-2010-00353) (to W.N.).

■ REFERENCES

(1) (a) Kovaleva, E. G.; Lipscomb, J. D. *Nat. Chem. Biol.* **2008**, *4*, 186. (b) Bruijnincx, P. C. A.; van Koten, G.; Klein Gebbink, R. J. M. *Chem. Soc. Rev.* **2008**, *37*, 2716. (c) Kryatov, S. V.; Rybak-Akimova, E. V. *Chem. Rev.* **2005**, *105*, 2175.

(2) (a) Galonic, D. P.; Barr, E. W.; Walsh, C. T.; Bollinger, J. M., Jr.; Krebs, C. *Nat. Chem. Biol.* **2007**, *3*, 113. (b) Krebs, C.; Fujimori, D. G.; Walsh, C. T.; Bollinger, J. M., Jr. *Acc. Chem. Res.* **2007**, *40*, 484.

(3) McQuilken, A. C.; Goldberg, D. P. *Dalton Trans.* **2012**, *41*, 10883.

(4) (a) Groves, J. T. *Proc. Natl. Acad. Sci. U.S.A.* **2003**, *100*, 3569. (b) van Eldik, R. *Coord. Chem. Rev.* **2007**, *251*, 1649.

(5) (a) Nam, W. *Acc. Chem. Res.* **2007**, *40*, 522. (b) Que, L., Jr. *Acc. Chem. Res.* **2007**, *40*, 493.

(6) (a) Cho, J.; Jeon, S.; Wilson, S. A.; Liu, L. V.; Kang, E. A.; Braymer, J. J.; Lim, M. H.; Hedman, B.; Hodgson, K. O.; Valentine, J. S.; Solomon, E. I.; Nam, W. *Nature* **2011**, *478*, 502. (b) Cho, J.; Sarangi, R.; Nam, W. *Acc. Chem. Res.* **2012**, *45*, 1321.

(7) Nam, W.; Lee, Y.-M.; Fukuzumi, S. *Acc. Chem. Res.* **2014**, *47*, 1146.

(8) Hohenberger, J.; Ray, K.; Meyer, K. *Nat. Commun.* **2012**, *3*, 720.

(9) (a) Lee, Y.-M.; Dhuri, S. N.; Sawant, S. C.; Cho, J.; Kubo, M.; Ogura, T.; Fukuzumi, S.; Nam, W. *Angew. Chem., Int. Ed.* **2009**, *48*, 1803. (b) Kotani, H.; Suenobu, T.; Lee, Y.-M.; Nam, W.; Fukuzumi, S. *J. Am. Chem. Soc.* **2011**, *133*, 3249.

(10) MacBeth, C. E.; Golombek, A. P.; Young, V. G., Jr.; Yang, C.; Kuczera, K.; Hendrich, M. P.; Borovik, A. S. *Science* **2000**, *289*, 938.

(11) (a) Ellis, W. C.; McDaniel, N. D.; Bernhard, S.; Collins, T. J. *J. Am. Chem. Soc.* **2010**, *132*, 10990. (b) Fillol, J. L.; Codola, Z.; Garcia-Bosch, I.; Gómez, L.; Pla, J. J.; Costas, M. *Nat. Chem.* **2011**, *3*, 807.

(12) (a) Chen, G.; Chen, L.; Ng, S.-M.; Man, W.-L.; Lau, T.-C. *Angew. Chem., Int. Ed.* **2013**, *52*, 1789. (b) Hong, D.; Mandal, S.; Yamada, Y.; Lee, Y.-M.; Nam, W.; Llobet, A.; Fukuzumi, S. *Inorg. Chem.* **2013**, *52*, 9522.

(13) Kim, S. O.; Sastri, C. V.; Seo, M. S.; Kim, J.; Nam, W. *J. Am. Chem. Soc.* **2005**, *127*, 4178.

(14) Hong, S.; Lee, Y.-M.; Shin, W.; Fukuzumi, S.; Nam, W. *J. Am. Chem. Soc.* **2009**, *131*, 13910.

(15) (a) Lee, Y.-M.; Hong, S.; Morimoto, Y.; Shin, W.; Fukuzumi, S.; Nam, W. *J. Am. Chem. Soc.* **2010**, *132*, 10668. (b) Comba, P.; Lee, Y.-M.; Nam, W.; Waleska, A. *Chem. Commun.* **2014**, *50*, 412.

(16) Thibon, A.; England, J.; Martinho, M.; Young, V. G., Jr.; Frisch, J. R.; Guillot, R.; Girerd, J.-J.; Münck, E.; Que, L., Jr.; Banse, F. *Angew. Chem., Int. Ed.* **2008**, *47*, 7064.

(17) Rohde, J.-U.; In, J.-H.; Lim, M. H.; Brennessel, W. W.; Bukowski, M. R.; Stubna, A.; Münck, E.; Nam, W.; Que, L., Jr. *Science* **2003**, *299*, 1037.

(18) Li, F.; Van Heuvelen, K. M.; Meier, K. K.; Münck, E.; Que, L., Jr. *J. Am. Chem. Soc.* **2013**, *135*, 10198.

(19) Bancroft, E. E.; Blount, H. N.; Janzen, E. G. *J. Am. Chem. Soc.* **1979**, *100*, 3692.

(20) Konishi, T.; Fujitsuka, M.; Ito, O.; Toba, Y.; Usui, Y. *J. Phys. Chem. A* **1999**, *103*, 9938.

(21) Lee, Y.-M.; Bang, S.; Kim, Y. M.; Cho, J.; Hong, S.; Nomura, T.; Ogura, T.; Troeppner, O.; Ivanovic-Burmazovic, I.; Sarangi, R.; Fukuzumi, S.; Nam, W. *Chem. Sci.* **2013**, *4*, 3917−3923.

(22) Lee, Y.-M.; Kotani, H.; Suenobu, T.; Nam, W.; Fukuzumi, S. *J. Am. Chem. Soc.* **2008**, *130*, 434.

(23) Fukuzumi, S.; Morimoto, Y.; Kotani, H.; Naumov, P.; Lee, Y.-M.; Nam, W. *Nat. Chem.* **2010**, *2*, 756.

(24) The yield of diphenylborinic acid was determined by the ^1H NMR peak at δ = 6.5 ppm due to the OH group of diphenylborinic acid, which exhibited a low field shift as compared to phenylboronic acid (Figures S1 and S2 in Supporting Information).

(25) Biphenyl was reported to be the only product after the treatment of the product solution by a flash column of alumina,[18] which could have eliminated phenol and other polar products.

(26) For autocatalytic formation of $[(TMC)Fe^{IV}(O)]^{2+}$ with isopropanol and O_2, see: Morimoto, Y.; Lee, Y.-M.; Nam, W.; Fukuzumi, S. *Chem. Commun.* **2013**, *49*, 2500.

(27) $Sc(OTf)_3$ has been reported to promote electron-transfer reactions from electron donors to electron acceptors when the radical anions of electron acceptors bind with $Sc(OTf)_3$; see refs 28−31.

(28) (a) Fukuzumi, S. *Prog. Inorg. Chem.* **2009**, *56*, 49. (b) Fukuzumi, S.; Ohkubo, K. *Coord. Chem. Rev.* **2010**, *254*, 372. (c) Fukuzumi, S. *Coord. Chem. Rev.* **2013**, *257*, 1564. (d) Fukuzumi, S.; Ohkubo, K.; Morimoto, Y. *Phys. Chem. Chem. Phys.* **2012**, *14*, 8472.

(29) (a) Fukuzumi, S.; Ohkubo, K. *Chem.—Eur. J.* **2000**, *6*, 4532. (b) Okamoto, K.; Imahori, H.; Fukuzumi, S. *J. Am. Chem. Soc.* **2003**,

125, 7014. (c) Fukuzumi, S.; Yuasa, J.; Suenobu, T. *J. Am. Chem. Soc.* **2002**, *124*, 12566. (d) Yuasa, J.; Suenobu, T.; Fukuzumi, S. *J. Am. Chem. Soc.* **2003**, *125*, 12090. (e) Fukuzumi, S.; Satoh, N.; Yuasa, J.; Ohkubo, K. *J. Am. Chem. Soc.* **2004**, *126*, 7585. (f) Yuasa, J.; Suenobu, T.; Fukuzumi, S. *ChemPhysChem* **2006**, *7*, 942.

(30) (a) Tsui, E. Y.; Kanady, J. S.; Agapie, T. *Inorg. Chem.* **2013**, *52*, 13833. (b) Tsui, E. Y.; Tran, R.; Yano, J.; Agapie, T. *Nat. Chem.* **2013**, *5*, 293. (c) Kanady, J. S.; Mendoza-Cortes, J. L.; Tsui, E. Y.; Nielsen, R. J.; Goddard, W. A.; Agapie, T. *J. Am. Chem. Soc.* **2013**, *135*, 1073.

(31) (a) Morimoto, Y.; Kotani, H.; Park, J.; Lee, Y.-M.; Nam, W.; Fukuzumi, S. *J. Am. Chem. Soc.* **2011**, *133*, 403. (b) Park, J.; Morimoto, Y.; Lee, Y.-M.; Nam, W.; Fukuzumi, S. *J. Am. Chem. Soc.* **2011**, *133*, 5236. (c) Yoon, H.; Lee, Y.-M.; Wu, X.; Cho, K.-B.; Pushkar, Y. N.; Nam, W.; Fukuzumi, S. *J. Am. Chem. Soc.* **2013**, *135*, 9186.

(32) Yu, T.; Lin, M. C. *J. Am. Chem. Soc.* **1994**, *116*, 9571.

(33) Tokmakov, I. V.; Kim, G.; Kislov, V. V.; Mebel, A. M.; Lin, M. C. *J. Phys. Chem. A* **2005**, *109*, 6114.

(34) Davis, A. G. *J. Chem. Res.* **2008**, 361.

(35) For radical chain autoxidation reactions, see: Rogério, A. F.; Tomás, R. A. F.; Bordado, J. C. M.; Gomes, J. F. P. *Chem. Rev.* **2013**, *113*, 7421.

(36) Fukuzumi, S.; Hironaka, K.; Tanaka, T. *J. Am. Chem. Soc.* **1983**, *105*, 4722.

(37) The concentration of O_2 in O_2-saturated MeCN at 298 K was determined to be 13 mM; see: Fukuzumi, S.; Mochizuki, S.; Tanaka, T. *Inorg. Chem.* **1989**, *28*, 2459.

(38) BPh_4^- was stable in the presence of Sc^{3+} without O_2. There was no spectral change of BPh_4^- in the presence of large excess Sc^{3+}.

(39) Fukuzumi, S.; Kuroda, S.; Tanaka, T. *J. Am. Chem. Soc.* **1985**, *107*, 3020.

(40) A similar decomposition of ROOH via a radical chain pathway has been reported; see: Fukuzumi, S.; Ono, Y. *J. Chem. Soc., Perkin Trans. 2* **1977**, 625.

(41) Meisters, M.; Vandeberg, J. T.; Cassaretto, F. P.; Posvic, H.; Moore, C. E. *Anal. Chim. Acta* **1970**, *49*, 481.

(42) The smaller yield (70%) of $[(TMC)Fe^{IV}(O)]^{2+}$ reported in refs 16 and 18 may result from the consumption of BPh_4^- before addition of $[(TMC)Fe^{II}]^{2+}$ because of the acid-promoted autoxidation of BPh_4^- with O_2.

(43) Brønsted acids have been reported to promote electron-transfer reactions from electron donors to electron acceptors when the radical anions of electron acceptors are protonated; see refs 44 and 45.

(44) (a) Fukuzumi, S.; Ishikawa, K.; Hironaka, K.; Tanaka, T. *J. Chem. Soc., Perkin Trans. 2* **1987**, 751. (b) Fukuzumi, S.; Mochizuki, S.; Tanaka, T. *J. Am. Chem. Soc.* **1989**, *111*, 1497. (c) Ishikawa, M.; Tanaka, T. *J. Chem. Soc., Perkin Trans. 2* **1989**, 1811. (d) Ishikawa, K.; Fukuzumi, S.; Goto, T.; Tanaka, T. *J. Am. Chem. Soc.* **1990**, *112*, 1577.

(45) (a) Fukuzumi, S.; Kotani, H.; Lee, Y.-M.; Nam, W. *J. Am. Chem. Soc.* **2008**, *130*, 15134. (b) Das, D.; Lee, Y.-M.; Ohkubo, K.; Nam, W.; Karlin, K. D.; Fukuzumi, S. *J. Am. Chem. Soc.* **2013**, *135*, 4018. (c) Park, J.; Lee, Y.-M.; Nam, W.; Fukuzumi, S. *J. Am. Chem. Soc.* **2013**, *135*, 5052.

(46) Armarego, W. L. F.; Chai, C. L. L. *Purification of Laboratory Chemicals*, 6th ed.; Elsevier: Oxford, U.K., 2009.

(47) *Organic Syntheses*; Saltzman, H., Sharefkin, J. G., Eds.; Wiley: New York, 1973; Collect. Vol. *V*, p 658.